Polymer Chemistry

ROYAL SOCIETY OF CHEMISTRY

PAPER

View Article Online
View Journal | View Issue

Cite this: *Polym. Chem.*, 2024, **15**, 4264

Heterogenous catalysis for oxygen tolerant photoredox atom transfer radical polymerization and small-molecule dehalogenation†

Kriti Kapil, [a] Mingkang Sun, [a] Ting-Chih Lin, [a] Hironobu Murata, [a] Grzegorz Szczepaniak, [b] Khidong Kim,[a] Stephen DiLuzio, [a] Jaepil Jeong, [a] Mitchell Baumer, [a] Stefan Bernhard, [a] Tomasz Kowalewski [a] and Krzysztof Matyjaszewski *[a]

Heterogeneous photocatalysts (PCs) have garnered attention for their sustainability and cost-effectiveness. Despite the existence of various types of these PCs, their synthesis often involves complex, multi-step procedures and laborious purification. Herein, we propose a simple method for attaching small-molecule photocatalytic species onto crosslinked 3-D polymer networks as insoluble scaffolds to create robust heterogeneous PCs. The highly swellable poly(ethylene glycol)-based ChemMatrix (CM) resin, known for its amphiphilic properties and high functional group loading, facilitated the covalent immobilization of the photoredox dye Eosin Y (EY), but also streamlined functionalization with Ir(III) complexes. The resulting heterogeneous CM-EY demonstrated efficient photocatalytic performance in open-to-air dual photoredox catalysis of atom transfer radical polymerization (photo-ATRP) under green light. This was confirmed by the well-controlled synthesis of polymers with molecular masses ranging from 20 kDa to 300 kDa and low dispersities. Furthermore, CM-EY exhibited excellent photostability and recyclability over multiple cycles of ATRP. The heterogeneous catalysis of photo-ATRP provided high temporal control and enabled benign conditions for synthesizing protein-polymer hybrids (PPH). When combined with the initiator-modified CM (CM-BIB), CM-EY facilitated the solid-phase synthesis of homopolymers and block copolymers with recyclable performance. However, the coordinatively bound Ir@CM showed decreased catalytic activity and efficiency toward photoredox dehalogenation due to the leaching of active species during recycling. This study highlights the advantages of the covalent linking of catalysts to solid supports over non-covalent interactions, underscoring the potential of functionalized polymer resin as a promising scaffold. Such an approach offers customization and tunability, presenting opportunities for innovation in green chemistry.

Received 18th August 2024,
Accepted 2nd October 2024

DOI: 10.1039/d4py00899e

rsc.li/polymers

Introduction

Photoredox catalysis (PCs) has emerged as a powerful tool in synthetic chemistry, allowing the activation of organic molecules under mild conditions through visible light absorption. This approach has changed organic transformations[1–3] and facilitated reversible deactivation radical polymerizations (RDRPs) for the synthesis of macromolecules and polymer bioconjugates.[4–14] While homogeneous PCs offer advantages like accessible catalytic sites and high selectivity,[14–18] recyclable heterogeneous PCs have gained prominence due to their versatility across various reaction mediums and cost-effectiveness.[19–22] These recyclable PCs can undergo multiple catalytic cycles without compromising activity or selectivity, aligning well with green chemistry principles.[23–25] Overall, the rational design of heterogeneous PCs represents a significant advancement, offering sustainable solutions and enhancing efficiency in various chemical processes.[13]

Photo-induced atom transfer radical polymerization (ATRP) has emerged as a commonly used technique in recent years due to its mild reaction conditions, ability to control polymerization temporally and spatially and oxygen tolerance.[10,26–37] ATRP, a reversible redox process typically catalyzed by Cu complexes, involves the transfer of a halogen atom from the

[a]*Department of Chemistry, Carnegie Mellon University, 4400 Fifth Avenue, Pittsburgh, PA 15213, USA. E-mail: km3b@andrew.cmu.edu, matyjaszewski@cmu.edu*
[b]*Faculty of Chemistry, University of Warsaw, Pasteura 1, 02-093 Warsaw, Poland*

†Electronic supplementary information (ESI) available: The details of experimental procedures, additional analysis, and polymerization results (PDF). See DOI: https://doi.org/10.1039/d4py00899e

dormant polymer chain end to the Cu^{I}/L activator, forming a propagating radical and X–Cu^{II}/L deactivator.[38–47] In classical photo-ATRP, light acts as an external stimulus to continuously regenerate the Cu^{I}/L activator in the presence of excess amine ligands.[45] In organocatalyzed ATRP (O-ATRP), the dormant polymer chain is directly activated by electron transfer from a PC in the excited state.[48,49] The dual catalysis systems use PCs to trigger and drive polymerization and copper complexes to control radical propagation.[17,18,50–53] In a recent study, we utilized a well-known xanthene dye, Eosin Y to perform a dual photoredox/copper-catalyzed ATRP under green light.[18] Eosin Y (EY) dye as an organic PC alongside a copper complex (X–Cu^{II}/L) at ppm levels, enabled efficient polymerization of methacrylates and acrylates under aerobic conditions with excellent temporal control.[18,54] This method allowed the rapid synthesis of well-defined hyperbranched polymers and polymer bioconjugates.[55–58] However, due to potential toxicity and coloration, the presence of PCs and transition metal catalysts in polymer products can pose challenges in various applications such as electronics, healthcare, and automotive.[59] Strategies such as precipitation, adsorption, degradation, and membrane separation are employed to remove catalysts.[60–62] Each method has its advantages and limitations depending on the specific characteristics of the PCs and the desired properties of the final polymer product.[63] The choice of removal method often depends on factors such as efficiency, cost-effectiveness, environmental impact, and scalability for industrial applications.[25,64]

Various types of heterogeneous PCs based on semiconductor nanoparticles,[65] up conversion nanoparticles,[66] nanocomposites,[67,68] metal–organic frameworks,[69] photoactive graphitic materials,[70,71] and conjugated covalent organic networks[72,73] have been developed. Their synthesis often involves complex processes and tedious purification steps, limiting scalability. To simplify this, integrating insoluble scaffolds with small-molecule photocatalytic species has been explored. Materials such as graphene and graphene oxides,[74] nanoparticles,[75] silica gels,[76] carbon fibers,[77,78] and polymers[6,19,20,79] are frequently utilized as catalyst supports to host photoactive moieties such as organic dyes or single-atom catalytic sites.[80] Nevertheless, the synthesis of these composite materials often entails harsh conditions, such as high-temperature pyrolysis, and may lead to catalyst aggregation. Additionally, rigid heterogeneous catalyst supports may restrict interactions between the photoactive sites and the reaction medium. To date, only modest molecular weights have been attained using heterogeneous PCs, which also lack compatibility in both organic and aqueous media.[4]

Polymer networks with 3D crosslinked architectures represent a vital class of functional soft materials.[81–84] Gels act as swollen polymer networks, bridging the gap between solids and liquids.[20,24] They have shown potential as heterogeneous catalyst supports due to their favorable swelling behaviors and flexibility.[20,24] ChemMatrix (CM), a poly(ethylene glycol) (PEG)-based network initially developed for the solid-phase synthesis of peptides[85,86] is comprised of thermally and chemically stable ether bonds. CM resin exhibits high swelling ratios in both organic solvents and aqueous media, with comparable functional group loading and easy product cleavage.[85,86] Recently, we reported CM resin functionalized with atom transfer radical polymerization (ATRP) initiators, enabling precise synthesis of multi-block copolymers directly from the solid support.[87] This successful ATRP initiation underscored CM's capability to mimic homogeneous initiators when swollen, facilitating facile interactions with polymerization components. Despite its widespread use in biology and biomedical engineering, CM's potential as a scaffold for catalysts remains relatively underexplored.[86,88–90]

In our study, we developed two heterogeneous photoactive materials based on CM-resin. Firstly, we covalently immobilized EY onto CM (CM-EY) for dual photoredox catalysis of ATRP. CM-EY demonstrated efficient photocatalytic performance, temporal control, and excellent photostability, ensuring prolonged catalytic activity over multiple cycles without degradation. Secondly, we anchored Ir(III) complexes onto ligand-functionalized CM (Ir@CM) through coordinative bonding. Ir@CM exhibited reduced efficiency and diminishing activity over successive cycles due to the leaching of active species. This study highlights the potential of functionalized polymer resin as a promising scaffold for catalyst immobilization due to its ease of separation. The importance of the covalent attachment of photocatalysts to solid supports and design principles and synthetic methodologies of these heterogeneous PCs are also discussed.

Results and discussion

Eosin-functionalized ChemMatrix (CM-AM-EY)

Synthesis and characterization. The photoredox dye EY was covalently immobilized onto amine ($-NH_2$) functionalized sites (0.5–0.7 mmol g^{-1}) of CM resin (CM-AM) using carbodiimide coupling in acetonitrile (ACN) (Scheme 1A). To prevent potential interference from free $-NH_2$ groups on CM-AM during polymerization, these sites were capped with acetic anhydride (see ESI†). Similarly, –OH functionalized CM resin (CM-HMPB) was also modified under the same conditions in dimethylformamide (DMF) (Scheme 1B). Following this, a thorough washing of the EY-immobilized CM resin was conducted to remove EY that was not covalently bound. Two types of fluorescent CM-EY resins were produced, differing in the type of linkages between the resin and EY. One with a more stable amide linkage (CM-AM-EY) and the second with a labile ester linkage (CM-HMPB-EY) (Scheme 1) prone to hydrolysis under aqueous conditions. These resins were stored at 4 °C and showed remarkable stability, remaining unchanged for over 24 months.

Following the immobilization process, a fluorescence intensity counts (FIC) assay was conducted to quantify the concentration of EY immobilized per gram of both CM-AM-EY and CM-HMPB-EY (see ESI Fig. S1–S4†). The results indicated the presence of 4.6 ± 1.1 μmol EY per g of CM-AM-EY and 0.32 ±

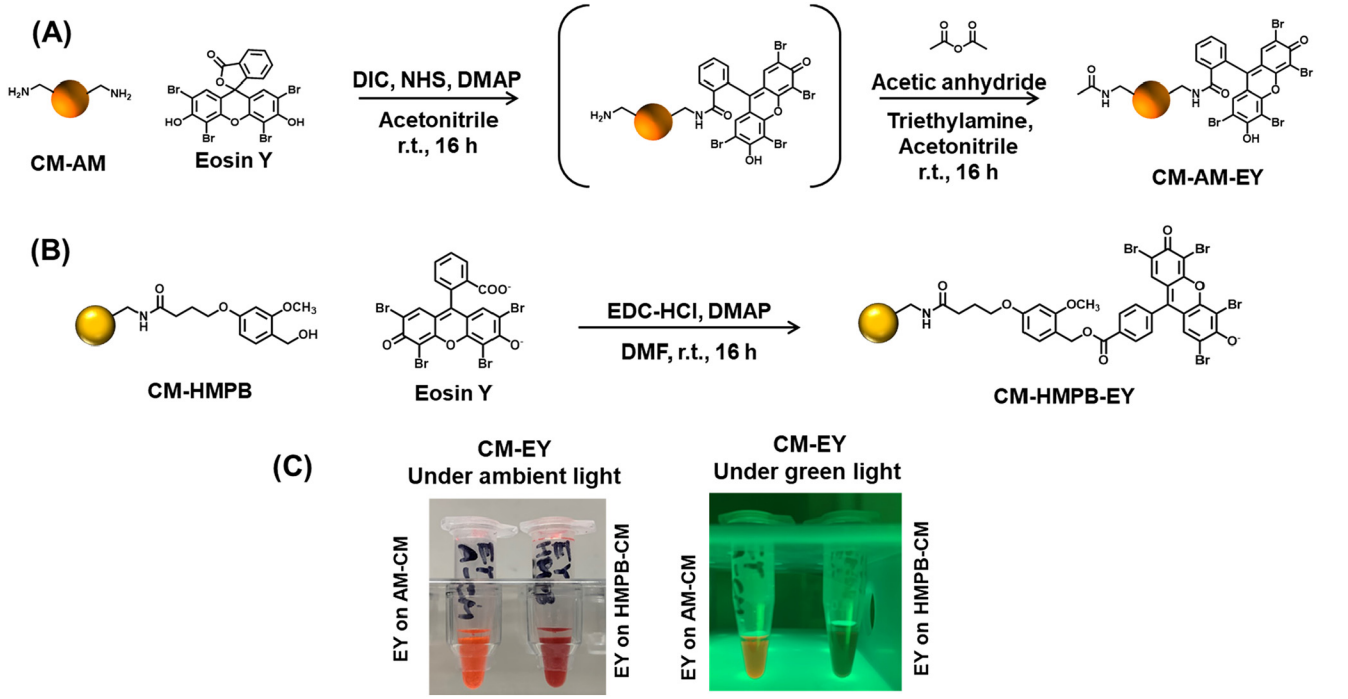

Scheme 1 Immobilization of EY on CM solid support. (A) Using amine ($-NH_2$) functionalized sites (0.5–0.7 mmol g^{-1}) of CM resin (CM-AM). (B) Using $-OH$ functionalized sites (0.4–0.6 mmol g^{-1}) CM resin (CM-HMPB). (C) Digital images of CM-AM-EY and CM-HMBP-EY under ambient conditions and green light irradiation.

0.06 μmol EY per g of CM-HMPB-EY. The digital images of the functionalized resins swollen in aqueous buffer under ambient conditions and green light irradiation revealed diminished fluorescence in the CM-HMPB-EY in contrast to CM-AM-EY (Scheme 1C). Despite using the same amount of EY for immobilization in both cases, the fluorescence intensity was 15 times lower for CM-HMPB-EY. This observation was counterintuitive as the CM resin shows better swelling performance in DMF, so better immobilization efficiency was expected. We hypothesized self-quenching of fluorescence in the CM-HMPB-EY due to the proximity of multiple EY molecules. Self-quenching of fluorescent dyes may occur due to non-covalent interactions such as π–π stacking or hydrophobic interactions. Furthermore, the Förster resonance energy transfer (FRET) mechanism could also lead to the non-radiative deactivation of the excited state of the dye molecules, resulting in reduced fluorescence intensity. To confirm our hypothesis, we cleaved the EY from CM-HMPB-EY support using 20% trifluoracetic acid (TFA) (see ESI, Scheme S1†). The actual concentration of immobilized dye was 150 ± 20 μmol EY per g CM. Using these estimations, we computed the distance between EY molecules in CM-AM-EY and CM-HMPB-EY. The calculations revealed the average distance between EY molecules in CM-AM-EY to be 15.3 nm and 4.8 nm in CM-HMPB-EY (see ESI†). Since Förster resonance energy transfer (FRET) can typically occur over distances up to 10 nm, these calculations suggest EY may be quenched in CM-HMPB-EY by FRET. It should be noted that this analysis assumes that EY is randomly distributed on the resin and does not aggregate. A more thorough characterization shall be needed to confirm the quenching phenomenon.

Optimization of heterogenous CM-AM-EY catalyzed photo ATRP

To verify the efficiency of CM-AM-EY to enable fully-oxygen tolerant dual photoredox/copper catalysis, oligo(ethylene glycol) methyl ether methacrylate (average M_n = 500, $OEOMA_{500}$) monomer was polymerized under green light (525 nm, 25.0 mW cm^{-2}) using 2-hydroxyethyl α-bromoisobutyrate (HOBIB) as the initiator, $CuBr_2$/TPMA (TPMA = tris(2-pyridyl methyl)amine) as the catalyst and CM-AM-EY resin as the heterogeneous photoredox catalyst. The polymerizations were conducted in 1× phosphate-buffered saline (PBS) with DMSO (10% v/v) in uncapped solid phase extraction (SPE) syringes equipped with 0.2 μm frits placed in a photo reactor with green LED lamp (525 nm, 25.0 mW cm^{-2}) at an ambient temperature maintained by a cooling fan. The polymerization reaction mixture was added to pre-weighed CM-AM-EY in an SPE cartridge and stirred at 500 rpm for 30 minutes, followed by irradiation for 30 minutes. After polymerization, the outlet of the syringe was uncapped, and the colorless, uncontaminated polymer sample was collected by simple vacuum filtration (Table 1).

In initial attempts, we performed heterogenous catalysis of photo ATRP using the previously optimized molar ratios ([$OEOMA_{500}$]/[HOBIB]/[CM-AM-EY]/[CuBr2]/[TPMA] = 200/1/

Table 1 Optimization of heterogenous CM-EY catalyzed photo ATRP

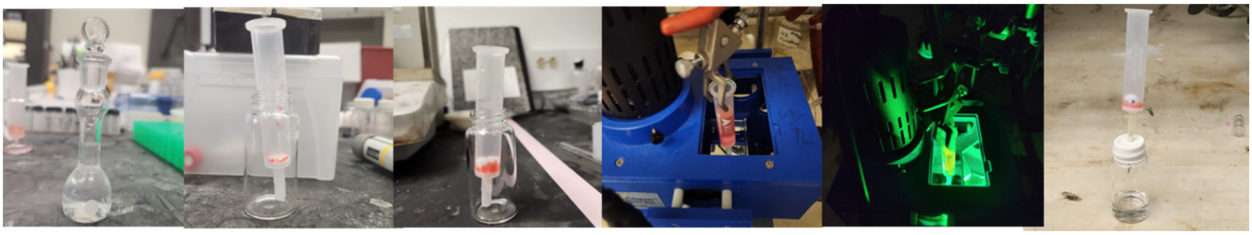

Entry	CM-catalyst	[CM-EY] μM	[TEOA] mM	α_M[a] (%)	$M_{n,th}$[b]	$M_{n,app}$[c]	$M_{n,abs}$[d]	$Đ$
1	CM-AM-EY	15	—	22%	22 000	12 500	16 800	1.16
2	CM-AM-EY	30	—	44%	44 000	22 500	32 400	1.13
3	CM-AM-EY	7.5	6.0	99%	99 000	60 900	94 500	1.15
4	CM-AM-EY	7.5	0.9	86%	86 000	58 500	88 200	1.17
5	CM-HMPB-EY	7.5	0.9	9%	9000	7600	9200	1.11
6	CM-HMPB-EY	7.5	3.0	88%	88 000	50 200	70 100	1.22

Reactions conditions: [OEOMA]/[HOBIB]/[CuBr2]/[TPMA]/[CM-AM-EY]/[TEOA]: 200/1/0.2/0.6/XX/XX, [$OEOMA_{500}$] = 300 mM, [HOBIB] = 1.5 mM, in 1× PBS buffer, irradiated for 30 min under green light LEDs (λ_{max} = 520 nm, 25.0 mW cm^{-2}), in an ambient atmosphere. Reaction volume 4.5 mL stirring at 500 rpm. [a] $OEOMA_{500}$ conversion was determined by using ^1H NMR spectroscopy. [b] Theoretical molecular weight was calculated using the equation $M_{n,th} = [M] \times MW_M \times \alpha M + MW_I$. [c] Apparent molecular weight ($M_{n,app}$) was analyzed by SEC using DMF as the eluent and PMMA as calibration standards. [d] $M_{n,abs}$ analyzed using SEC run using 1× PBS as eluent equipped with triple detectors: multi-angle light scattering (MALS), refractive index (RI), and UV detector.

0.01/0.2/0.6) (Table 1, entry 1). However, the monomer conversion after 30 minutes of irradiation, as analyzed by ^1H NMR, was considerably lower (22%) compared to the previously reported 84% conversion of monomer under identical conditions using homogeneous EY as the photoredox catalyst.[18] To enhance the polymerization rate, we doubled the molar ratio of CM-AM-EY (Table 1, entry 2). Although this adjustment led to an improvement in the overall monomer conversion after 30 minutes (44%), it remained relatively low, resulting in a significant amount of unreacted monomer in the final product.

The proposed mechanism from dual photoredox/copper catalysis suggested the oxidative quenching of excited state EY as the preferred pathway. Additionally, it highlighted the critical role of excess ligands in reducing the oxidized EY and closing the photocatalytic cycle.[14] We envisioned that the addition of excess triethanolamine (TEOA), a more cost-effective alkylamine, as a sacrificial electron donor would accelerate the overall polymerization kinetics. Heterogenous CM-AM-EY catalyzed photo ATRP was then performed in the presence of 3 mM of triethanolamine (TEOA), resulting in quantitative monomer conversion (>99%) and the SEC analysis revealed the absolute molecular weight ($M_{n,abs}$) of the polymer was slightly lower than the theoretical value ($M_{n,th}$) (Table 1, entry 3). Next, to enhance control, the polymerization was conducted with reduced amounts of CM-AM-EY and TEOA using molar ratios ([$OEOMA_{500}$]/[HOBIB]/[CM-AM-EY]/[CuBr2]/[TPMA]/[TEOA]) = 200/1/0.005/0.2/0.6/0.6 still resulted in a high monomer conversion and the synthesized $POEOMA_{500}$ showed good agreement between theoretical and absolute molecular weight and a narrow molecular weight distribution (Table 1, entry 4). Therefore, these optimized conditions using CM-AM-EY were used in all the subsequent polymerizations.

CM-HMPB-EY was also tested for heterogeneous catalysis of photo ATRP and revealed lower catalytic efficiency than its counterpart CM-AM-EY (Table 1, entry 5). Using an excess of amines (TEOA) accelerated the rate of polymerization reaching quantitative monomer conversion. However, poor agreement between $M_{n,th}$, and $M_{n,abs}$ was observed (Table 1, entry 6).

Kinetics of heterogeneous CM-AM-EY catalyzed photo ATRP

The kinetic analysis of heterogeneous CM-AM-EY catalyzed photo ATRP under optimized conditions ([$OEOMA_{500}$]/[HOBIB]/[CM-AM-EY]/[CuBr2]/[TPMA]/[TEOA]) = 200/1/0.005/0.2/0.6/0.6 revealed a linear first-order relationship between ln ($[M]_0/[M]_t$) and time. A short induction period of 5 min was followed by a rapid polymerization that reached 90% monomer conversion within 40 min (Fig. 1A). In addition, the molecular weights increased as a function of monomer conversion (Fig. 1B), and molecular weight distribution values remained low ($Đ \leq 1.17$) during the polymerization (Fig. 1C).

Varying the targeted degree of polymerization (DP)

Polymers with varying molecular weights were synthesized by adjusting the degree of polymerization (DP) through systematic variation of HOBIB initiator concentration (6 mM to 0.30 mM), while maintaining constant polymerization conditions ([$OEOMA_{500}$] = 300 mM, [CM-AM-EY] = 7.5 μM, [$CuBr_2$] = 0.3 mM, [TPMA] = 0.9 mM, [TEOA] = 0.9 mM). For a broad DP range (50–800), monomer conversions reached ≥70% within 30 minutes, yielding polymers with narrow molecular weight distributions ($Đ$ = 1.08–1.28) (Table 2, entries 1–5). At DP = 1000, conversion slightly decreased (66%), accompanied by a minor loss in molecular weight control (Table 2, entry 6). SEC traces exhibited symmetry without tailing or high molecular

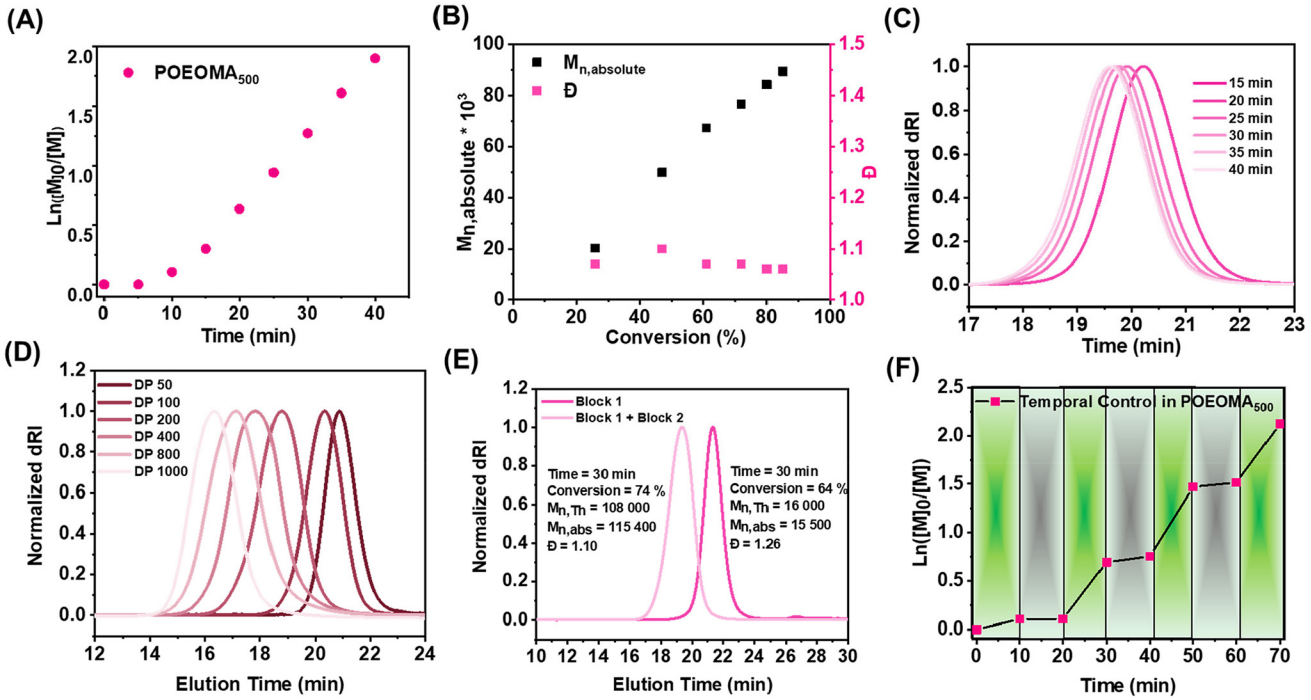

Fig. 1 Features of heterogenous CM-AM-EY catalyzed photo ATRP (A) first-order kinetics plot, (B) evolution of MW and *Đ* with conversion of monomer, (C) SEC traces shift to lower elution time, (D) SEC traces of polymers with varying molecular weights, (E) *in situ* chain extension and (F) temporal control.

Table 2 Varying targeted degrees of polymerization (DP)

Entry	[M]/[I]/[CM-AM-EY]/[$CuBr_2$]/[TPMA]/[TEOA]	[I] (mM)	Conv.[a] (%)	$M_{n,th}$[b]	$M_{n,abs}$[c]	*Đ*
1	50/1/0.0025/0.05/0.15/0.15	6.0	89	22 250	27 800	1.08
2	100/1/0.005/0.1/0.3/0.3	3.0	88	44 000	52 400	1.05
3	200/1/0.01/0.2/0.6/0.6	1.5	86	86 000	92 200	1.05
4	400/1/0.02/0.4/1.2/1.2	0.75	82	164 000	172 800	1.08
5	800/1/0.04/0.8/2.4/2.4	0.375	72	288 000	235 000	1.28
6	1000/1/0.05/1.0/3.0/3.0	0.30	66	330 000	280 400	1.42

Reactions conditions: [M]/[HOBIB]/[$CuBr_2$]/[TPMA]/[CM-AM-EY]/[TEOA]: 200/1/0.2/0.6/0.005/0.6, [M] = [$OEGMA_{500}$] = 300 mM, [HOBIB] = 6–0.30 mM, [TEOA] = 0.9 mM in 1× PBS buffer at rt, irradiated for 30 min under green light LEDs (λ_{max} = 520 nm, 25.0 mW cm^{-2}), stirring at 500 rpm in an ambient atmosphere. [a] $OEOMA_{500}$ conversion was determined by using ^{1}H NMR spectroscopy. [b] Theoretical molecular weight was calculated using the equation $M_{n,th} = [M] \times MW_M \times \alpha M + MW_I$. [c] $M_{n,abs}$ analyzed using SEC run using 1× PBS as eluent equipped with triple detectors: multiangle light scattering (MALS), refractive index (RI), and UV detector.

weight shoulders, highlighting the robustness of the CM-AM-EY-catalyzed photo-ATRP system (Fig. 1D).

In situ chain extension

The chain-end fidelity was confirmed by performing an *in situ* chain extension experiment. The first block of $POEOMA_{500}$ was synthesized with molar ratios [$OEOMA_{500}$]/[HOBIB]/[CM-AM-EY]/[CuBr2]/[TPMA]/[TEOA]: 50/1/0.0025/0.05/0.15/0.15 (conv. = 64%, $M_{n,abs}$ = 15 500, *Đ* = 1.26). $POEOMA_{500}$ was then used as a macroinitiator (macro-I) to graft the second block with target DP = 250. The polymerization was irradiated for 30 minutes resulting in a chain-extended $POEOMA_{500}$ (conv. = 74%, $M_{n,abs}$ = 115 400, *Đ* = 1.10). The SEC analysis showed a clear shift of the chain-extended polymer trace toward higher molecular weight without any shoulder or tailing at lower molecular weight, indicating high end-group fidelity (Fig. 1E).

Temporal control

To demonstrate temporal control in the heterogenous CM-AM-EY catalyzed photo ATRP, the polymerization mixture was subjected to intermittent light exposure with continued stirring at 500 rpm. The heterogeneous catalytic system showed high temporal control (Fig. 1F). Sustained polymerization was observed upon irradiation under green light while the dark periods halted the polymerization instantly and effec-

tively. Despite multiple cycles of light on and off periods for 70 minutes, the SEC trace of the final polymer sample showed well-controlled polymerization (conv. = 92%, $M_{n,abs}$ = 95 900, $Đ$ = 1.16) (Fig. S6†).

Reusability of CM-AM-EY

A notable characteristic of the heterogeneous CM-EY photocatalyst was its facile separation from the reaction mixture, allowing for repeated use in multiple ATRP cycles while maintaining its photocatalytic efficiency (Fig. 2A). The recycling of the CM-EY photocatalyst facilitated successive ATRP reactions of $OEOMA_{500}$ in the presence of the $CuBr_2$/TPMA catalyst. Following each polymerization cycle, the heterogenous solid-supported photocatalyst was easily isolated through simple filtration, washed multiple times with HPLC-grade water, and dried before being employed in the subsequent cycle. Across five cycles, high monomer conversions were achieved, resulting in polymers with well-controlled molecular weights and low dispersity values (Fig. 2B). Importantly, no degradation in the photocatalyst's performance or contamination of the polymer by EY was observed throughout the recycling process (Fig. S7†). Furthermore, the immobilized CM-EY displayed enhanced photostability as compared to free EY under the same irradiation conditions (Fig. S8A and B†).

From aqueous to organic media to expand monomer scope

The monomer scope was expanded to include hydrophilic methacrylates known for their biocompatibility, such as carboxy betaine methacrylate (CBMA), (methylsulfinyl)ethyl methacrylate (MSEMA), and methacrylate with a shorter poly (ethylene glycol) unit ($OEOMA_{300}$). The resulting polymers – $POEOMA_{300}$, PCBMA, and PMSEMA, synthesized *via* heterogeneous CM-EY photo-ATRP exhibited predictable molecular weights and low dispersity (Table S1,† entries 1–3, Fig. 3A–C). For polyacrylates, the combination of Cu/Me_6Tren and CM-EY photocatalyst yielded well-controlled $POEOA_{480}$ (Table S1,† entry 4 and Fig. 3D).

Leveraging the excellent swelling behavior of CM-EY in both polar and organic solvents, we performed CM-EY catalyzed photo-ATRP in organic media using triethylamine (TEA) as the excess electron donor (Table S1,† entries 5 and 6). Polymerizations of methyl acrylate (MA) and ethyl acrylate (EA) in DMSO were conducted at room temperature under green light (525 nm, 25.0 mW cm^{-2}) for 120 min in capped SPE cartridges to prevent volatile monomer loss. Stirring at 750 rpm without deoxygenation, the resulting PMA and PEA exhibited narrow molecular weight distributions and predictable molecular weights (Fig. 3E and F).

Protein-polymer hybrids (PPH) by heterogenous CM-EY catalyzed photo ATRP

Protein-polymer hybrids represent a versatile class of biomaterials that combine the unique catalytic activity of proteins with the tunable properties of synthetic polymers.[8,91–94] These hybrids have garnered significant interest across various disciplines, including biomedicine, materials science, and biotechnology.[95] Leveraging the benefit of homogenous catalysis enabled by heterogenous CM-EY towards PPH has the potential to simplify the purification of polymer bioconjugates,[96,97] resulting in more cost-effective synthetic processes and greater industrial relevance.[5]

Therefore, we functionalized two different proteins, namely bovine serum albumin (BSA) and chymotrypsin (CT) with ATRP initiators to prepare BSA-$iBBr_{22}$ and CT-$iBBr_{12}$ respectively. BSA was chosen due to its relatively higher resilience while CT is a therapeutic enzyme used to treat pancreatic insufficiency. Grafting-from ATRP was used to graft PCBMA polymers from the protein's surface using heterogenous CM-EY as the photocatalyst. The SEC-MALS analysis of

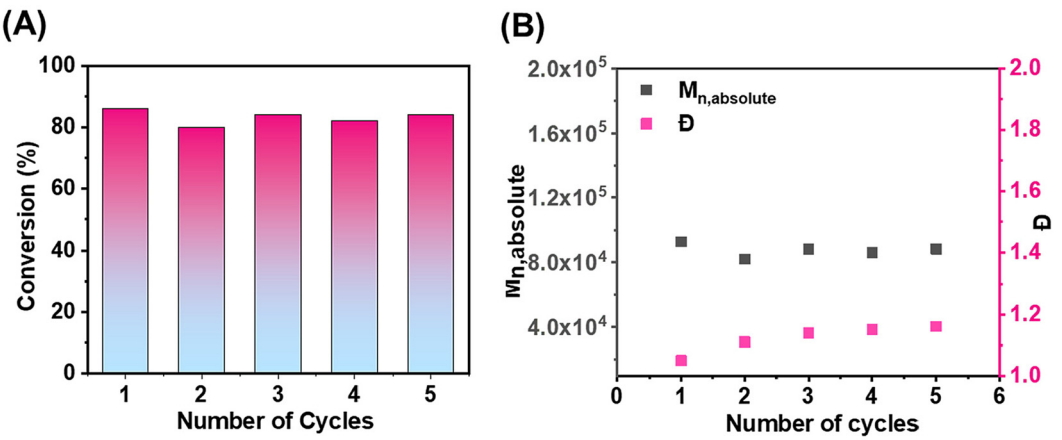

Fig. 2 Recycling of heterogenous CM-EY a photocatalyst in ATRP of $OEOMA_{500}$ showing retention of photocatalytic activity over multiple cycles. (A) Monomer conversion and (B) molecular weight ($M_{n,abs}$, black) and dispersity ($Đ$, pink) of the resulting polymers in recycling experiments. Reaction conditions: ([$OEOMA_{500}$]/[HOBIB]/[CM-EY]/[$CuBr_2$]/[TPMA]/[TEOA]) = 200/1/0.005/0.2/0.6/0.6 in 1× PBS under green light irradiation (525 nm, 25 mW cm^{-2}), CM-AM-EY = 1.6 mg mL^{-1}.

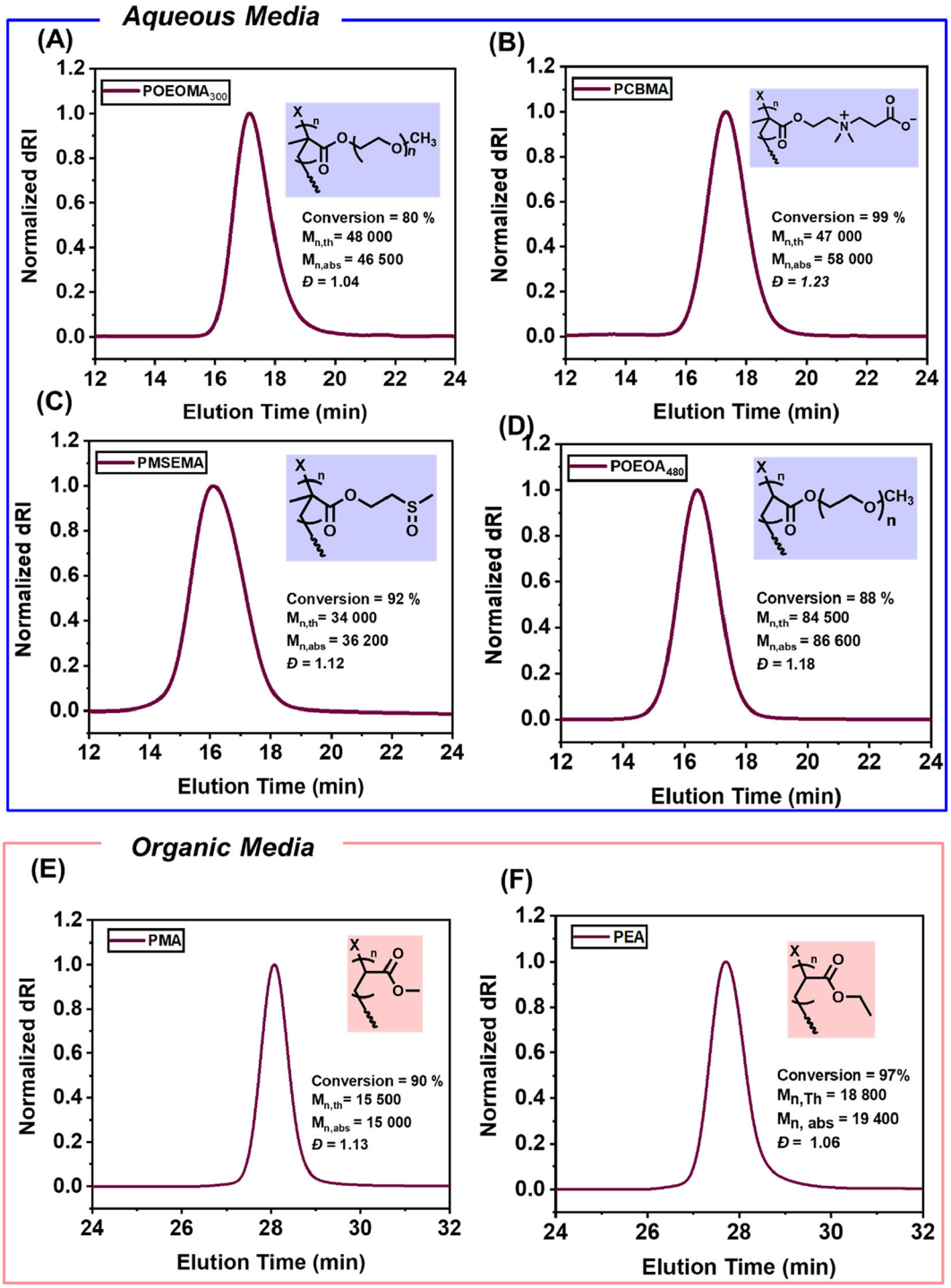

Fig. 3 Expanding monomer scope of heterogenous CM-EY catalyzed photo ATRP to (A) $POEOMA_{300}$, (B) PCBMA, (C) PMSEMA, (D) $POEOA_{480}$, (E) PMA and (F) PEA.

the synthesized bioconjugates showed monomodal distribution and higher absolute molecular weights of the bioconjugates as compared to native proteins, indicating a successful grafting-from ATRP (Fig. 4A and B). The larger dispersities could be related to variable number of initiators anchored to proteins.

Solid-phase polymer synthesis by heterogenous CM-EY catalyzed photo ATRP

We recently demonstrated that the remarkable swelling capability of CM resin facilitated the solid-phase synthesis of multiblock copolymers without the need for cumbersome and was-

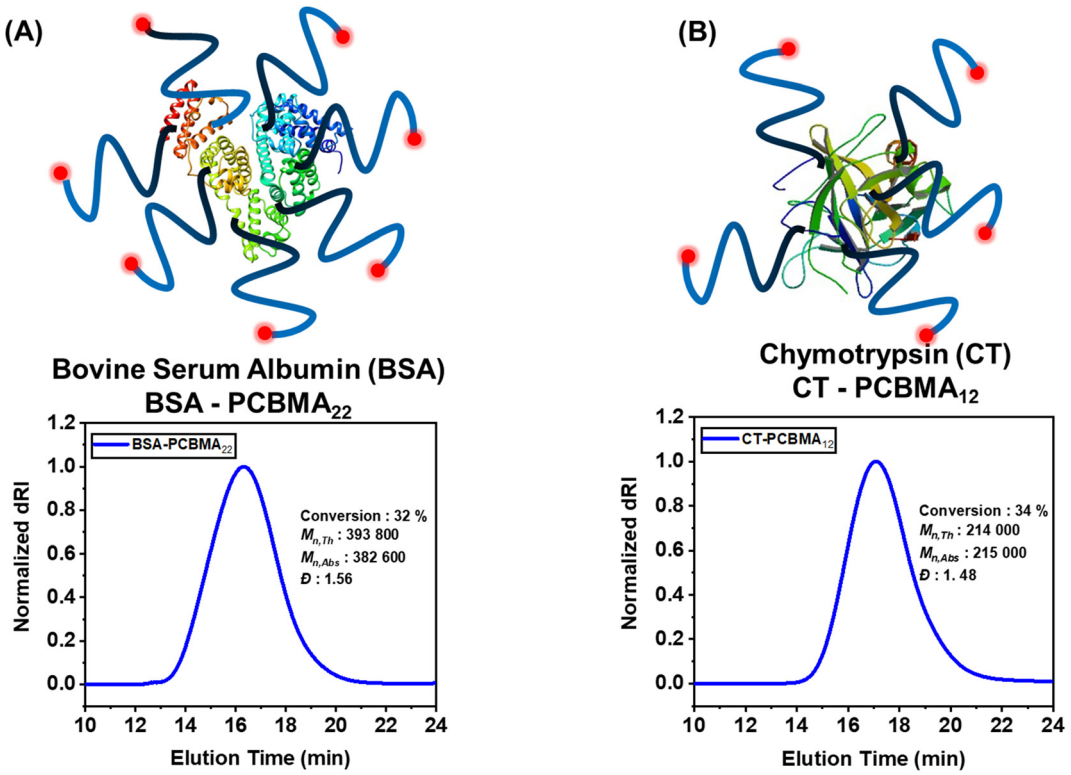

Fig. 4 Synthesis of protein–polymer hybrids (PPH) by heterogenous CM-EY catalyzed photo-ATRP (A) BSA-PCBMA$_{22}$ and (B) CT-PCBMA$_{12}$. Reaction conditions: ([CBMA]/[Proetin-I]/[CM-EY]/[$CuBr_2$]/[TPMA]/[TEOA]) = 200/1/0.005/0.2/0.6/0.6 in 1× PBS under green light irradiation (525 nm, 25 mW cm^{-2}), CM-EY = 1.6 mg mL^{-1}.

teful purification steps between each block synthesis.[87] Here, by employing heterogeneous CM resin functionalized with ATRP initiators (CM-BIB), we facilitated the solid-supported synthesis of polymers *via* photo ATRP using CM-AM-EY as the photocatalyst. This system uniquely integrates both ATRP initiator moieties and the PC (*i.e.*, EY) onto a solid-support CM (Fig. 5). CM-BIB is composed of an ester linkage between hydroxy-functionalized CM and the ATRP initiator, while CM-AM-EY features an amide linkage between amine-functionalized CM and EY. The controlled ATRP process is governed by the interactions of the growing polymer chain end with a small-molecule catalyst ($Cu^{II}Br_2$/L), which can diffuse into the crosslinked network of the CM resin, thus ensuring high chain-end fidelity.[98]

MA monomer was grafted from the CM-BIB in DMSO at room temperature using heterogeneous CM-EY as the photocatalyst and Cu/Me_6Tren as the co-catalyst, ethyl α-bromoisobutyrate (EBIB) was used as the homogenous sacrificial initiator in the system. After 60 minutes of irradiation of the polymerization reaction in capped SPE cartridge under green light LEDs (λ_{max} = 525 nm, 25.0 mW cm^{-2}), the polymerization mixture was separated from the heterogenous solid supports. ^{1}H NMR of the solution phase showed 50% conversion of [MA] monomer achieved. 20% TFA/H_2O was used to cleave the ester bond on CM-BIB releasing the grafted PMA. SEC analysis of PMA revealed that the polymerization proceeded with a high-control over molecular weight and dispersity in both solution and solid-phase (Fig. 5A).

To demonstrate one-pot synthesis of block copolymer on the solid support, the CM- grafted with PMA was thoroughly washed with DMSO and, without further purification, mixed with the next monomer [EA], Cu/Me6Tren as the co-catalyst, and EBIB initiator. The polymerization mixture was irradiated for 60 min to graft PMA-*b*-PEA block copolymer from the CM resin. The acid-cleaved PMA-*b*-PEA block copolymer revealed clear shifting in the SEC trace towards high molecular weight ($M_{n,abs}$ = 15000, $Đ$ = 1.26) without any shoulder, indicating successful chain extension on solid support was achieved (Fig. 5B).

Furthermore, utilizing an orthogonal linkage strategy to synthesize CM-BIB and CM-AM-EY enabled the recycling of this heterogeneous solid-support combination for subsequent ATRP reactions. The mixture of CM-grafted PMA and CM-AM-EY was subjected to acid hydrolysis (20% TFA/H_2O), thoroughly washed with DMSO, and re-functionalized with the ATRP initiator. During acid hydrolysis, CM-BIB releases the PMA, while CM-AM-EY remains unchanged. The re-functionalized CM-BIB resin and CM-EY mixture was successfully used for subsequent solid-phase photo ATRP, demonstrating the versatility of the solid-supported ATRP initiator and photocatalyst (Fig. 5C). However, SEC traces revealed a slightly lower molecular weight of cleaved PMA compared to solution-phase

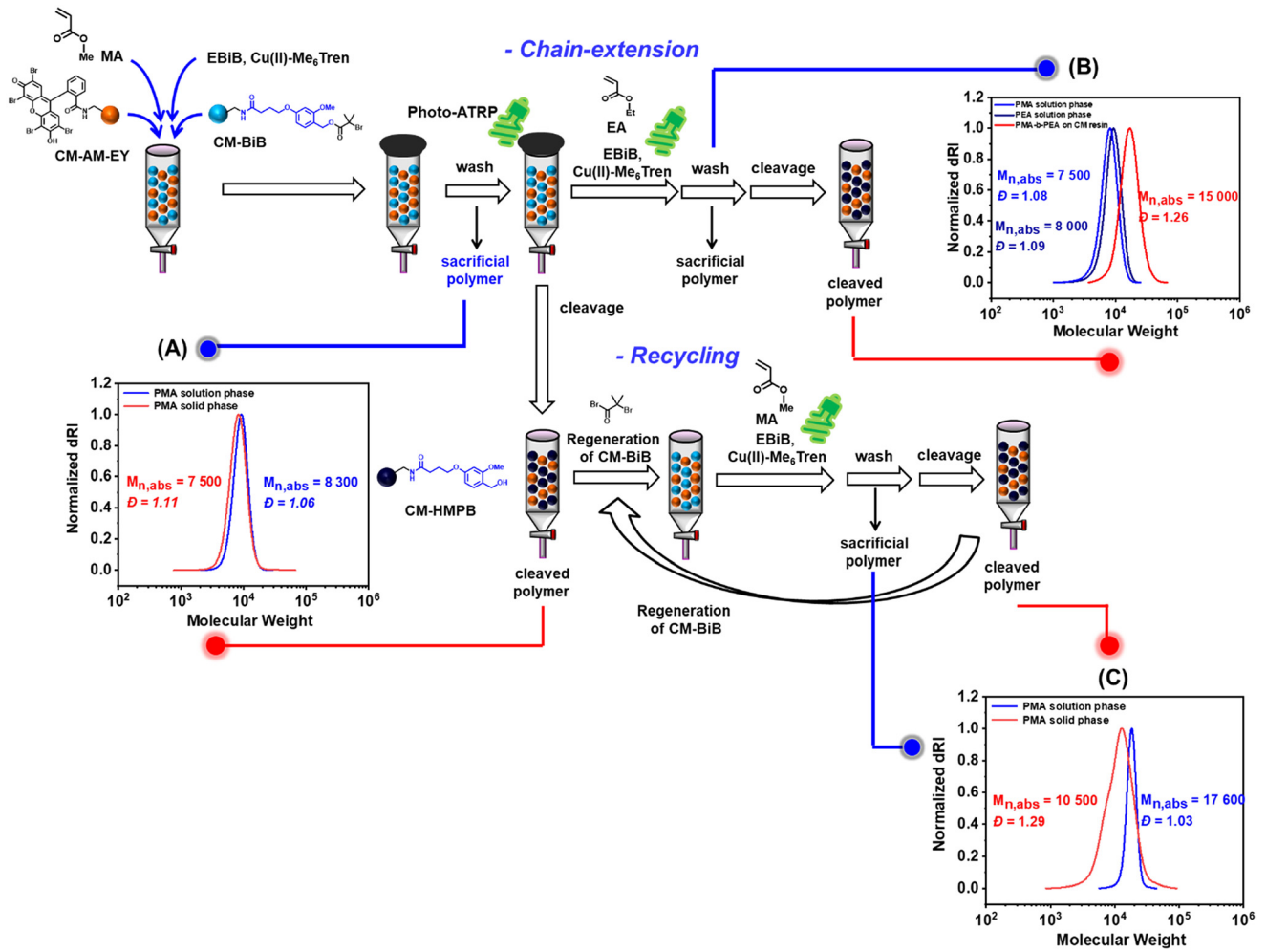

Fig. 5 (A) Solid-phase synthesis of polymers catalyzed by heterogenous CM-AM-EY (A) homopolymer of PMA grafted from CM-BIB, (B) block copolymer of PMA-*b*-PEA grafted from CM-BIB and (C) recycling of CM-BIB and CM-AM-EY for solid-phase polymer synthesis.

PMA, likely due to incomplete PMA cleavage from the previous step, resulting in sample contamination during recycling. This underscores the necessity of efficient TFA cleavage before recycling. Overall, this work highlights the ability to selectively cleave and reattach polymer chains from CM-BIB containing ester linkages while maintaining the amide linkages in CM-AM-EY intact.

Ir(III)-functionalized ChemMatrix (Ir@CM)

Encouraged by the successful photo ATRP achieved by CM-AM-EY, we sought to expand the scope of CM-based heterogeneous PC to other photocatalytic moieties such as transition metals. Therefore, we attempted to immobilize Ir(III) complexes through coordinative bonding and investigated the catalytic activity under blue light.

Photoluminescent cyclometalated iridium(III) complexes are promising photoactive compounds for their highly tunable excited state properties *via* ligand manipulation,[99–102] as well as for their wide applications in sensors,[103] probing,[104] optoelectronics[101,105] and photoredox catalysis.[106–108] Particularly, heteroleptic $[Ir(C^N)_2(N^N)]^+$ complexes (where C^N refers to 2-phenylpyridyl-type ligands, and N^N refers to 1,2-diimine-type ligands) have been widely studied due to their enhanced photostability and long-lived triplet excited state caused by spin–orbital couplings and rapid intersystem crossing (ISC).[109] Thus, photoactive Ir^{III} complexes have been used to catalyze various types of photoredox reactions, such as hydrogen evolution,[107,110] water reduction,[106,111] dehalogenation[112] as well as photoinduced polymerizations.[113–115]

Streamlined "continuous-flow" synthesis of Ir@CM

The photoluminescent Ir@CM was obtained by functionalizing a commercially available hydroxy-terminated CM resin using a streamlined, "continuous-flow"-like setup in a solid-phase extraction (SPE) syringe, that enabled the multistep functionalization without tedious purification. The iodination of the –OH group was first performed based on a reported procedure,[116] followed by the azidation[117] and Cu-catalyzed azide–alkyne cycloaddition forming 2-triazol-pyridine-type (N^N) ligand.[118] The removal of small-molecule side products and

excess reactants was performed by simply washing the resin with solvents multiple times (see ESI†).

The final ligand coordinated Ir(III) complexes (L-Ir@CM) on CM resins were synthesized using two Ir(III) complexes composed of different C^N ligands, namely 2-phenylpyridine (ppy) and 2-(4-(trifluoromethyl)phenyl)benzo[*d*]thiazole (pbtz). Ir dimers containing the ppy or pbtz ligand were first synthesized *via* the reaction between $IrCl_3$ and the corresponding C^N ligand (Scheme S2†). Then, Ir dimers were reacted with CM functionalized with 2-triazol-pyridine (CM-L, L = ligand) and yielded ppy-Ir@CM or pbtz-Ir@CM (Scheme S3†).[99,107,110] As shown in Fig. 6, dried ppy-Ir@CM and pbtz-Ir@CM resins showed distinctive green and orange solid-state photoluminescence (λ_{ext} = 365 nm), respectively, indicating the successful attachment of the Ir complexes. The thiazole-based Ir complexes are known to exhibit interesting photophysical properties,[119] as described below.

Characterization and photophysical properties of Ir@CM

Fourier Transform Infrared (FTIR) spectroscopy confirmed the presence of C–F bonds at 1033 cm^{-1} and C–S bonds at 754 cm^{-1} within pbtz-Ir (see Fig. S9(A)†). Thermogravimetric analysis (TGA) conducted on pbtz-Ir@CM in air revealed a residual weight of 2.83 wt% at 800 °C, with a secondary decomposition occurring around 360 °C, attributed to the estimated 2.4 wt% of Ir(III) complex present based on residual weight (see Fig. S9(B)†). The swelling characteristics remained largely unaffected following the functionalization of Ir moieties (see Fig. S9(C)†).

Photophysical properties were assessed using UV-vis and photoluminescence, comparing the native CM resin to pbtz-CM-Ir (see Fig. S9(D and E)). A notable difference in photophysical attributes between the two materials was observed. The additional absorption and excitation peaks detected the original tethered iridium complex excitation. A model compound (see Fig. S10†) was synthesized for comparative analysis of the photoactivity of pbtz-Ir@CM. Excited state lifetime measurements demonstrated a fourfold reduction in lifetime upon immobilization, compared to the model compound (Table S2†). This decrease was ascribed to vibrational motions within the CM matrix, which elevate the relaxation rate of the excited state.

To further validate the photophysical properties of these relatively unusual Ir^{III} complexes, the excited state properties

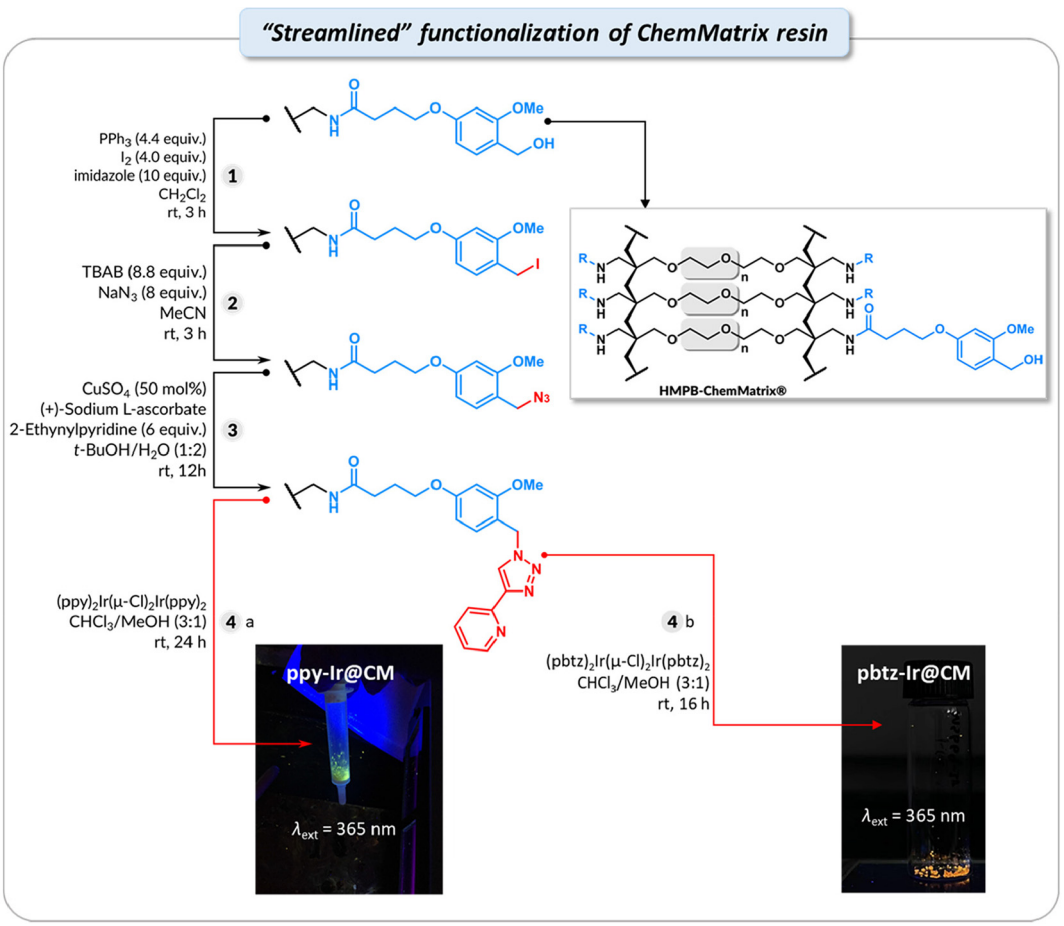

Fig. 6 Synthesis of ppy-Ir@CM and pbtz-Ir@CM *via* the "streamlined" functionalization of ChemMatrix. ppy = phenyl-pyridine, pbtz = 2-(4-(trifluoromethyl)phenyl)benzo[d]thiazole, TBAB = tetrabutylammonium bromide.

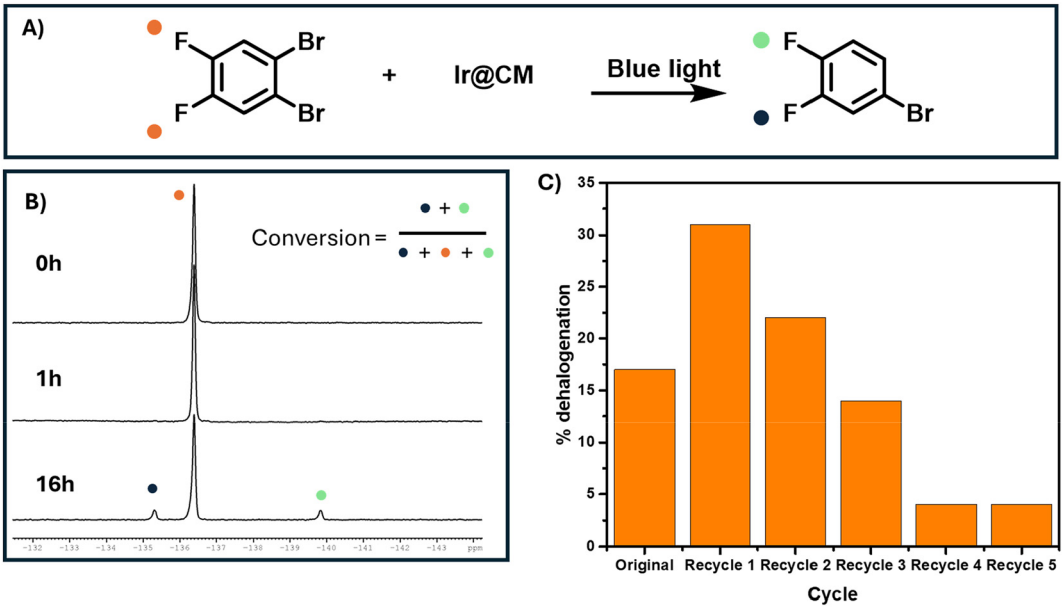

Fig. 7 (A) Reaction scheme of dehalogenation; (B) ^{19}F NMR of reaction mixture at different time points. Debromination is indicated by the appearance of two peaks at −135.25 ppm and −139.75 ppm. (C) Dehalogenation efficiency of pbtz-Ir@CM over numerous cycles determined by integration of peaks at −135.25 ppm and −139.75 ppm against 1,2-dibromo-4,5-difluorobenzene peak at −136.4 ppm.

of a model Ir complex containing the same C^N and N^N ligands were studied by density functional theory (DFT) calculations, which revealed a locally excited triplet state and explained the origin of the vibronic patterns observed in the emission spectra (Fig. S11†).

Investigation of catalytic performance

To probe the catalytic activity of pbtz-Ir@CM, we performed dehalogenation of 1,2-dibromo-4,5-difluorobenzene, which can be easily monitored *via* ^{19}F NMR. Following a previously reported method, pbtz-Ir@CM was used as a heterogeneous catalyst for debromination under blue light. After 1 hour, no change could be observed in the reaction solution (Fig. 7A). At 16 h, the peaks around −135.25 and −139.75 ppm emerged, indicating successful debromination of a single bromine (Fig. 7B). The second bromine proved harder to remove, as the loss of an electron-withdrawing group resulted in an increased oxidation potential for the remaining bromine. These peaks were then integrated against the original peak at −136.25 ppm to determine the dehalogenation efficiency of 17% (Fig. 7C).

The catalyst was then recycled five times until dehalogenation was no longer observed (Fig. 7C). After the first cycle, dehalogenation efficiency increased. This is explained by the pulverization of the pbtz-Ir@CM, increasing the surface area of the catalyst, allowing for more efficient dehalogenation. On subsequent cycles, a progressive decrease in dehalogenation efficiency was observed. This was mainly attributed to the leaching of the iridium complex, as the solutions showed slight discoloration after the reaction and photobleaching of the compound.

Comparison between covalent *vs.* non-covalent attachment of photocatalyst

In conclusion, this study demonstrates that the covalent linkage between the photocatalyst EY and the solid support (CM-EY) offers numerous advantages over non-covalent interactions (Ir@CM), which are more prone to disruption, potentially leading to catalyst leaching from the support. This enhanced stability significantly reduces the risk of catalyst detachment or deactivation during reactions, resulting in improved performance and longevity, as evidenced by the efficient recycling of CM-AM-EY for photo ATRP. Moreover, covalent attachment effectively prevents photocatalyst aggregation, thus minimizing photobleaching.

Furthermore, the precise positioning and orientation of the catalyst on the solid support enabled by covalent attachment may enhance its interaction with reactants, thereby improving catalytic efficiency and selectivity. In contrast, non-covalent interactions may lack the precise control necessary for optimal catalyst orientation and positioning. Covalent linkage also yields a more robust catalyst-support system, facilitating easier separation and recycling of the catalyst post-reaction. This aspect is crucial for cost reduction and waste minimization.

Moreover, covalent linkage offers greater flexibility for tailoring the properties of the catalyst-support system, such as adjusting loading density or introducing specific functional groups. This capability allows for fine-tuning of catalytic performance to meet the requirements of various reactions or applications. Overall, covalent linkage between a catalyst and a solid support provides a more stable, efficient, and versatile platform for heterogeneous catalysis compared to non-covalent bonding interactions.

Author contributions

The manuscript was written through the contributions of all authors. All authors have given approval to the final version of the manuscript.

Data availability

The authors confirm that the data supporting the findings of this study are available within the article and/or its ESI.†

Conflicts of interest

The authors declare no competing interests.

Acknowledgements

This work was supported by NSF DMR 2202747, DMR 2324168, CHE 2404433, and DoE ER 45998.

References

1 X. Yang and D. Wang, Photocatalysis: From Fundamental Principles to Materials and Applications, *ACS Appl. Energy Mater.*, 2018, **1**, 6657–6693, DOI: **10.1021/acsaem.8b01345**.
2 E. R. McClure, P. Das, K. B. Idrees, D. Jung, O. K. Farha and J. A. Kalow, Photoredox Diels-Alder ladder polymerization, *Polym. Chem.*, 2023, **14**, 4906–4911, DOI: **10.1039/d3py00833a**.
3 S. Gisbertz and B. Pieber, Heterogeneous Photocatalysis in Organic Synthesis, *ChemPhotoChem*, 2020, **4**, 454–454, DOI: **10.1002/cptc.202000014**.
4 Z. X. An, S. L. Zhu and Z. S. An, Heterogeneous photocatalytic reversible deactivation radical polymerization, *Polym. Chem.*, 2021, **12**, 2357–2373, DOI: **10.1039/d1py00130b**.
5 R. A. Olson, A. B. Korpusik and B. S. Sumerlin, Enlightening advances in polymer bioconjugate chemistry: light-based techniques for grafting to and from biomacromolecules, *Chem. Sci.*, 2020, **11**, 5142–5156, DOI: **10.1039/d0sc01544j**.
6 R. A. Olson, J. S. Levi, G. M. Scheutz, J. J. Lessard, C. A. Figg, M. N. Kamat, K. B. Basso and B. S. Sumerlin, Macromolecular Photocatalyst for Synthesis and Purification of Protein-Polymer Conjugates, *Macromolecules*, 2021, **54**, 4880–4888, DOI: **10.1021/acs.macromol.1c00508**.
7 S. E. Averick, S. K. Dey, D. Grahacharya, K. Matyjaszewski and S. R. Das, Solid-phase incorporation of an ATRP initiator for polymer-DNA biohybrids, *Angew. Chem., Int. Ed.*, 2014, **53**, 2739–2744, DOI: **10.1002/ange.201308686**.
8 C. Cummings, H. Murata, R. Koepsel and A. J. Russell, Tailoring enzyme activity and stability using polymer-based protein engineering, *Biomaterials*, 2013, **34**, 7437–7443, DOI: **10.1016/j.biomaterials.2013.06.027**.
9 L. Fu, Z. Wang, S. Lathwal, A. E. Enciso, A. Simakova, S. R. Das, A. J. Russell and K. Matyjaszewski, Synthesis of Polymer Bioconjugates via Photoinduced Atom Transfer Radical Polymerization under Blue Light Irradiation, *ACS Macro Lett.*, 2018, **7**, 1248–1253, DOI: **10.1021/acsmacrolett.8b00609**.
10 X. C. Pan, M. A. Tasdelen, J. Laun, T. Junkers, Y. Yagci and K. Matyjaszewski, Photomediated controlled radical polymerization, *Prog. Polym. Sci.*, 2016, **62**, 73–125, DOI: **10.1016/j.progpolymsci.2016.06.005**.
11 D. J. Siegwart, J. K. Oh and K. Matyjaszewski, ATRP in the design of functional materials for biomedical applications, *Prog. Polym. Sci.*, 2012, **37**, 18–37, DOI: **10.1016/j.progpolymsci.2011.08.001**.
12 Y. Sun, S. Lathwal, Y. Wang, L. Y. Fu, M. Olszewski, M. Fantin, A. E. Enciso, G. Szczepaniak, S. Das and K. Matyjaszewski, Preparation of Well-Defined Polymers and DNA-Polymer Bioconjugates via Small-Volume eATRP in the Presence of Air, *ACS Macro Lett.*, 2019, **8**, 603–609, DOI: **10.1021/acsmacrolett.9b00159**.
13 C. Y. Wu, N. Corrigan, C. H. Lim, W. J. Liu, G. Miyake and C. Boyer, Rational Design of Photocatalysts for Controlled Polymerization: Effect of Structures on Photocatalytic Activities, *Chem. Rev.*, 2022, **122**, 5476–5518, DOI: **10.1021/acs.chemrev.1c00409**.
14 J. Xu, S. Shanmugam, H. T. Duong and C. Boyer, Organophotocatalysts for photoinduced electron transfer-reversible addition-fragmentation chain transfer (PET-RAFT) polymerization, *Polym. Chem.*, 2015, **6**, 5615–5624, DOI: **10.1039/c4py01317d**.
15 J. P. Cole, C. R. Federico, C. H. Lim and G. M. Miyake, Photoinduced Organocatalyzed Atom Transfer Radical Polymerization Using Low ppm Catalyst Loading, *Macromolecules*, 2019, **52**, 747–754, DOI: **10.1021/acs.macromol.8b02688**.
16 D. J. Cole-Hamilton, Homogeneous catalysis - new approaches to catalyst separation, recovery, and recycling, *Science*, 2003, **299**, 1702–1706, DOI: **10.1126/science.1081881**.
17 X. L. Hu, G. Szczepaniak, A. Lewandowska-Andralojc, J. Jeong, B. D. Li, H. Murata, R. G. Yin, A. M. Jazani, S. R. Das and K. Matyjaszewski, Red-Light-Driven Atom Transfer Radical Polymerization for High-Throughput Polymer Synthesis in Open Air, *J. Am. Chem. Soc.*, 2023, **145**, 24315–24327, DOI: **10.1021/jacs.3c09181**.
18 G. Szczepaniak, J. Jeong, K. Kapil, S. Dadashi-Silab, S. S. Yerneni, P. Ratajczyk, S. Lathwal, D. J. Schild, S. R. Das and K. Matyjaszewski, Open-air green-light-driven ATRP enabled by dual photoredox/copper catalysis, *Chem. Sci.*, 2022, **13**, 11540–11550, DOI: **10.1039/d2sc04210j**.
19 K. Bell, S. Freeburne, A. Wolford and C. W. Pester, Reusable polymer brush-based photocatalysts for PET-RAFT polymerization, *Polym. Chem.*, 2022, **13**, 6120–6126, DOI: **10.1039/d2py00966h**.

20 M. Chen, S. H. Deng, Y. W. Gu, J. Ling, M. J. MacLeod and J. K. Johnson, Logic-Controlled Radical Polymerization with Heat and Light: Multiple-Stimuli Switching of Polymer Chain Growth via a Recyclable, Thermally Responsive Gel Photoredox Catalyst, *J. Am. Chem. Soc.*, 2017, **139**, 2257–2266, DOI: **10.1021/jacs.6b10345**.

21 S. Faucher and S. P. Zhu, Fundamentals and development of high-efficiency supported catalyst systems for atom transfer radical polymerization, *J. Polym. Sci., Part A: Polym. Chem.*, 2007, **45**, 553–565, DOI: **10.1002/pola.21785**.

22 M. A. Fox and M. T. Dulay, Heterogeneous Photocatalysis, *Chem. Rev.*, 1993, **93**, 341–357, DOI: **10.1021/cr00017a016**.

23 P. Anastas and N. Eghbali, Green Chemistry: Principles and Practice, *Chem. Soc. Rev.*, 2010, **39**, 301–312, DOI: **10.1039/b918763b**.

24 S. Dadashi-Silab, F. Lorandi, M. J. DiTucci, M. K. Sun, G. Szczepaniak, T. Liu and K. Matyjaszewski, Conjugated Cross-linked Phenothiazines as Green or Red Light Heterogeneous Photocatalysts for Copper-Catalyzed Atom Transfer Radical Polymerization, *J. Am. Chem. Soc.*, 2021, **143**, 9630–9638, DOI: **10.1021/jacs.1c04428**.

25 S. Dworakowska, F. Lorandi, A. Gorczynski and K. Matyjaszewski, Toward Green Atom Transfer Radical Polymerization: Current Status and Future Challenges, *Adv. Sci.*, 2022, **9**, 2106076, DOI: **10.1002/advs.202106076**.

26 C. Aydogan, G. Yilmaz, A. Shegiwal, D. M. Haddleton and Y. Yagci, Photoinduced Controlled/Living Polymerizations, *Angew. Chem., Int. Ed.*, 2022, **61**, e202117377, DOI: **10.1002/anie.202117377**.

27 M. Chen, M. J. Zhong and J. A. Johnson, Light-Controlled Radical Polymerization: Mechanisms, Methods, and Applications, *Chem. Rev.*, 2016, **116**, 10167–10211, DOI: **10.1021/acs.chemrev.5b00671**.

28 S. Dadashi-Silab, S. Doran and Y. Yagci, Photoinduced Electron Transfer Reactions for Macromolecular Syntheses, *Chem. Rev.*, 2016, **116**, 10212–10275, DOI: **10.1021/acs.chemrev.5b00586**.

29 S. Dadashi-Silab, I. H. Lee, A. Anastasaki, F. Lorandi, B. Narupai, N. D. Dolinski, M. L. Allegrezza, M. Fantin, D. Konkolewicz, C. J. Hawker and K. Matyjaszewski, Investigating Temporal Control in Photoinduced Atom Transfer Radical Polymerization, *Macromolecules*, 2020, **53**, 5280–5288, DOI: **10.1021/acs.macromol.0c00888**.

30 S. Dadashi-Silab and K. Matyjaszewski, Temporal Control in Atom Transfer Radical Polymerization Using Zerovalent Metals, *Macromolecules*, 2018, **51**, 4250–4258, DOI: **10.1021/acs.macromol.8b00698**.

31 K. Parkatzidis, N. P. Truong, K. Matyjaszewski and A. Anastasaki, Photocatalytic ATRP Depolymerization: Temporal Control at Low ppm of Catalyst Concentration, *J. Am. Chem. Soc.*, 2023, **145**, 21146–21151, DOI: **10.1021/jacs.3c05632**.

32 Z. H. Wang, X. C. Pan, J. J. Yan, S. Dadashi-Silab, G. J. Xie, J. N. Zhang, Z. H. Wang, H. S. Xia and K. Matyjaszewski, Temporal Control in Mechanically Controlled Atom Transfer Radical Polymerization Using Low ppm of Cu Catalyst, *ACS Macro Lett.*, 2017, **6**, 546–549, DOI: **10.1021/acsmacrolett.7b00152**.

33 W. Q. Yan, S. Dadashi-Silab, K. Matyjaszewski, N. D. Spencer and E. M. Benetti, Surface-Initiated Photoinduced ATRP: Mechanism, Oxygen Tolerance, and Temporal Control during the Synthesis of Polymer Brushes, *Macromolecules*, 2020, **53**, 2801–2810, DOI: **10.1021/acs.macromol.0c00333**.

34 M. K. Yazdi, P. Zarrintaj, M. R. Saeb, M. Mozafari and S. A. Bencherif, Progress in ATRP-derived materials for biomedical applications, *Prog. Mater. Sci.*, 2024, **143**, 101248, DOI: **10.1016/j.pmatsci.2024.101248**.

35 X. C. Pan, M. Fantin, F. Yuan and K. Matyjaszewski, Externally controlled atom transfer radical polymerization, *Chem. Soc. Rev.*, 2018, **47**, 5457–5490, DOI: **10.1039/C8CS00259B**.

36 H. Feng, Z. Chen, L. Li, X. Shao, W. Fan, C. Wang, L. Song, K. Matyjaszewski, X. Pan and Z. Wang, Aerobic mechanochemical reversible-deactivation radical polymerization, *Nat. Commun.*, 2024, **15**, 6179, DOI: **10.1038/s41467-024-50562-z**.

37 N. Li and X. Pan, Controlled Radical Polymerization: from Oxygen Inhibition and Tolerance to Oxygen Initiation, *Chin. J. Polym. Sci.*, 2021, **39**, 1084–1092, DOI: **10.1007/s10118-021-2597-9**.

38 C. Fang, M. Fantin, X. C. Pan, K. de Fiebre, M. L. Coote, K. Matyjaszewski and P. Liu, Mechanistically Guided Predictive Models for Ligand and Initiator Effects in Copper-Catalyzed Atom Transfer Radical Polymerization (Cu-ATRP), *J. Am. Chem. Soc.*, 2019, **141**, 7486–7497, DOI: **10.1021/jacs.9b02158**.

39 C. Y. Lin, M. L. Coote, A. Gennaro and K. Matyjaszewski, Ab initio evaluation of the thermodynamic and electrochemical properties of alkyl halides and radicals and their mechanistic implications for atom transfer radical polymerization, *J. Am. Chem. Soc.*, 2008, **130**, 12762–12774, DOI: **10.1021/ja8038823**.

40 F. Lorandi, M. Fantin, H. Jafari, A. Gorczynski, G. Szczepaniak, S. Dadashi-Silab, A. A. Isse and K. Matyjaszewski, Reactivity Prediction of Cu-Catalyzed Halogen Atom Transfer Reactions Using Data-Driven Techniques, *J. Am. Chem. Soc.*, 2023, **145**, 21587–21599, DOI: **10.1021/jacs.3c07711**.

41 F. Lorandi, M. Fantin and K. Matyjaszewski, Atom Transfer Radical Polymerization: A Mechanistic Perspective, *J. Am. Chem. Soc.*, 2022, **144**, 15413–15430, DOI: **10.1021/jacs.2c05364**.

42 K. Matyjaszewski, Future Directions for Atom Transfer Radical Polymerizations, *Chem. Mater.*, 2024, **36**, 1775–1778, DOI: **10.1021/acs.chemmater.3c03213**.

43 K. Matyjaszewski, Current status and outlook for ATRP, *Eur. Polym. J.*, 2024, **11**, 113001, DOI: **10.1016/j.eurpolymj.2024.113001**.

44 T. E. Patten and K. Matyjaszewski, Atom transfer radical polymerization and the synthesis of polymeric materials,

Adv. Mater., 1998, **10**, 901–915, DOI: **10.1002/(sici)1521-4095(199808)10:12<901::aid-adma901>3.3.co;2-2**.

45 T. G. Ribelli, D. Konkolewicz, S. Bernhard and K. Matyjaszewski, How are radicals (re)generated in photochemical ATRP?, *J. Am. Chem. Soc.*, 2014, **136**, 13303–13312, DOI: **10.1021/ja506379s**.

46 T. G. Ribelli, F. Lorandi, M. Fantin and K. Matyjaszewski, Atom Transfer Radical Polymerization: Billion Times More Active Catalysts and New Initiation Systems, *Macromol. Rapid Commun.*, 2019, **40**, 1800616, DOI: **10.1002/marc.201800616**.

47 J. S. Wang and K. Matyjaszewski, Controlled/"Living" Radical Polymerization. Halogen Atom Transfer Radical Polymerization Promoted by a Cu(I)/Cu(II) Redox Process, *Macromolecules*, 1995, **28**, 7901–7910, DOI: **10.1021/ma00127a042**.

48 D. A. Corbin and G. M. Miyake, Photoinduced Organocatalyzed Atom Transfer Radical Polymerization (O-ATRP): Precision Polymer Synthesis Using Organic Photoredox Catalysis, *Chem. Rev.*, 2022, **122**, 1830–1874, DOI: **10.1021/acs.chemrev.1c00603**.

49 X. C. Pan, C. Fang, M. Fantin, N. Malhotra, W. Y. So, L. A. Peteanu, A. A. Isse, A. Gennaro, P. Liu and K. Matyjaszewskit, Mechanism of Photoinduced Metal-Free Atom Transfer Radical Polymerization: Experimental and Computational Studies, *J. Am. Chem. Soc.*, 2016, **138**, 2411–2425, DOI: **10.1021/jacs.5b13455**.

50 S. Dadashi-Silab, K. Kim, F. Lorandi, G. Szczepaniak, S. Kramer, L. Peteanu and K. Matyjaszewski, Red-Light-Induced, Copper-Catalyzed Atom Transfer Radical Polymerization, *ACS Macro Lett.*, 2022, **11**, 376–381, DOI: **10.1021/acsmacrolett.2c00080**.

51 X. L. Hu, R. G. Yin, J. Jeong and K. Matyjaszewski, Robust Miniemulsion PhotoATRP Driven by Red and Near-Infrared Light, *J. Am. Chem. Soc.*, 2024, **146**, 13417–13426, DOI: **10.1021/jacs.4c02553**.

52 A. M. Jazani, D. J. Schild, J. Sobieski, X. L. Hu and K. Matyjaszewski, Visible Light-ATRP Driven by Tris(2-Pyridylmethyl)Amine (TPMA) Impurities in the Open Air, *Macromol. Rapid Commun.*, 2023, **44**, 2200855, DOI: **10.1002/marc.202200855**.

53 M. K. Sun, G. Szczepaniak, S. Dadashi-Silab, T. C. Lin, T. Kowalewski and K. Matyjaszewski, Cu-Catalyzed Atom Transfer Radical Polymerization: The Effect of Cocatalysts, *Macromol. Chem. Phys.*, 2023, **224**, 2200347, DOI: **10.1002/macp.202200347**.

54 K. Kapil, A. M. Jazani, G. Szczepaniak, H. Murata, M. Olszewski and K. Matyjaszewski, Fully Oxygen-Tolerant Visible-Light-Induced ATRP of Acrylates in Water: Toward Synthesis of Protein-Polymer Hybrids, *Macromolecules*, 2023, **56**, 2017–2026, DOI: **10.1021/acs.macromol.2c02537**.

55 K. Kapil, A. M. Jazani, J. Sobieski, L. P. Madureira, G. Szczepaniak, M. R. Martinez, A. Gorczynski, H. Murata, T. Kowalewski and K. Matyjaszewski, Hydrophilic Poly(meth)acrylates by Controlled Radical Branching Polymerization: Hyperbranching and Fragmentation, *Macromolecules*, 2024, **57**, 5368–5379, DOI: **10.1021/acs.macromol.4c00408**.

56 K. Kapil, H. Murata, G. Szczepaniak, A. J. Russell and K. Matyjaszewski, Tailored Branched Polymer–Protein Bioconjugates for Tunable Sieving Performance, *ACS Macro Lett.*, 2024, **13**, 461–467, DOI: **10.1021/acsmacrolett.4c00059**.

57 K. Kapil, G. Szczepaniak, M. R. Martinez, H. Murata, A. M. Jazani, J. Jeong, S. R. Das and K. Matyjaszewski, Visible–Light–Mediated Controlled Radical Branching Polymerization in Water, *Angew. Chem., Int. Ed.*, 2023, **62**, e202217658, DOI: **10.1002/anie.202217658**.

58 K. Kapil, S. R. Xu, I. S. Lee, H. Murata, S. J. Kwon, J. S. Dordick and K. Matyjaszewski, Highly Sensitive Detection of Bacteria by Binder-Coupled Multifunctional Polymeric Dyes, *Polymers*, 2023, **15**, 2723, DOI: **10.3390/polym15122723**.

59 K. Parkatzidis, H. S. Wang, N. P. Truong and A. Anastasaki, Recent Developments and Future Challenges in Controlled Radical Polymerization: A 2020 Update, *Chem*, 2020, **6**, 1575–1588, DOI: **10.1016/j.chempr.2020.06.014**.

60 S. Faucher, P. Okrutny and S. P. Zhu, Facile and effective purification of polymers produced by atom transfer radical polymerization via simple catalyst precipitation and microfiltration, *Macromolecules*, 2006, **39**, 3–5, DOI: **10.1021/ma051920a**.

61 K. Matyjaszewski, T. Pintauer and S. Gaynor, Removal of copper-based catalyst in atom transfer radical polymerization using ion exchange resins, *Macromolecules*, 2000, **33**, 1476–1478, DOI: **10.1021/ma9911445**.

62 J. C. Maxwell, B. C. Baker and C. F. J. Faul, Controlled Removal of Organic Dyes from Aqueous Systems Using Porous Cross-Linked Conjugated Polyanilines, *ACS Appl. Polym. Mater.*, 2023, **5**, 662–671, DOI: **10.1021/acsapm.2c01718**.

63 K. A. Chism, D. A. Corbin and G. M. Miyake, Removal of photoredox catalysts from polymers synthesized by organocatalyzed atom transfer radical polymerization, *J. Polym. Sci.*, 2022, **60**, 2747–2755, DOI: **10.1002/pol.20220320**.

64 G. Szczepaniak, L. Y. Fu, H. Jafari, K. Kapil and K. Matyjaszewski, Making ATRP More Practical: Oxygen Tolerance, *Acc. Chem. Res.*, 2021, **54**, 1779–1790, DOI: **10.1021/acs.accounts.1c00032**.

65 S. Dadashi-Silab, M. A. Tasdelen, A. M. Asiri, S. B. Khan and Y. Yagci, Photoinduced Atom Transfer Radical Polymerization Using Semiconductor Nanoparticles, *Macromol. Rapid Commun.*, 2014, **35**, 454–459, DOI: **10.1002/marc.201300704**.

66 W. J. Zhang, J. H. He, C. N. Lv, Q. Y. Wang, X. C. Pang, K. Matyjaszewski and X. C. Pan, Atom Transfer Radical Polymerization Driven by Near-Infrared Light with Recyclable Upconversion Nanoparticles, *Macromolecules*, 2020, **53**, 4678–4684, DOI: **10.1021/acs.macromol.0c00850**.

67 A. Bansal, A. Kumar, P. Kumar, S. Bojja, A. K. Chatterjee, S. S. Ray and S. L. Jain, Visible light-induced surface

initiated atom transfer radical polymerization of methyl methacrylate on titania/reduced graphene oxide nanocomposite, *RSC Adv.*, 2015, **5**, 21189–21196, DOI: **10.1039/c4ra15615c**.

68 Y. M. Huang, Y. F. Zhu and E. Egap, Semiconductor Quantum Dots as Photocatalysts for Controlled Light-Mediated Radical Polymerization, *ACS Macro Lett.*, 2018, **7**, 184–189, DOI: **10.1021/acsmacrolett.7b00968**.

69 L. W. Zhang, G. Ng, N. Kapoor-Kaushik, X. B. Shi, N. Corrigan, R. Webster, K. Jung and C. Boyer, 2D Porphyrinic Metal-Organic Framework Nanosheets as Multidimensional Photocatalysts for Functional Materials, *Angew. Chem., Int. Ed.*, 2021, **60**, 22664–22671, DOI: **10.1002/anie.202107457**.

70 B. Kiskan, J. S. Zhang, X. C. Wang, M. Antonietti and Y. Yagci, Mesoporous Graphitic Carbon Nitride as a Heterogeneous Visible Light Photoinitiator for Radical Polymerization, *ACS Macro Lett.*, 2012, **1**, 546–549, DOI: **10.1021/mz300116w**.

71 L. Zhou, Z. Q. Zhang, M. M. Li, Q. Wang, J. N. Gao, K. B. Li and L. Lei, Graphitic carbon nitride (g-C_3N_4) as a sustainable heterogeneous photocatalyst for metal free and oxygen-tolerant photo-atom transfer radical polymerization (photo-ATRP), *Green Chem.*, 2021, **23**, 9617–9624, DOI: **10.1039/d1gc03604a**.

72 D. D. Medina, T. Sick and T. Bein, Photoactive and Conducting Covalent Organic Frameworks, *Adv. Energy Mater.*, 2017, **7**, 201700387, DOI: **10.1002/aenm.201700387**.

73 M. K. Sun, F. Lorandi, R. Yuan, S. Dadashi-Silab, T. Kowalewski and K. Matyjaszewski, Assemblies of Polyacrylonitrile-Derived Photoactive Polymers as Blue and Green Light Photo-Cocatalysts for Cu-Catalyzed ATRP in Water and Organic Solvents, *Front. Chem.*, 2021, **9**, 734076, DOI: **10.3389/fchem.2021.734076**.

74 Z. Li, W. F. Zhang, Q. S. Zhao, H. Y. Gu, Y. Li, G. L. Zhang, F. B. Zhang and X. B. Fan, Eosin Y Covalently Anchored on Reduced Graphene Oxide as an Efficient and Recyclable Photocatalyst for the Aerobic Oxidation of α-Aryl Halogen Derivatives, *ACS Sustainable Chem. Eng.*, 2015, **3**, 468–474, DOI: **10.1021/sc5006654**.

75 S. Shanmugam, S. H. Xu, N. N. M. Adnan and C. Boyer, Heterogeneous Photocatalysis as a Means for Improving Recyclability of Organocatalyst in "Living" Radical Polymerization, *Macromolecules*, 2018, **51**, 779–790, DOI: **10.1021/acs.macromol.7b02215**.

76 V. Blanchard, Z. Asbai, K. Cottet, G. Boissonnat, M. Port and Z. Amara, Continuous Flow Photo-oxidations Using Supported Photocatalysts on Silica, *Org. Process Res. Dev.*, 2020, **24**, 822–826, DOI: **10.1021/acs.oprd.9b00420**.

77 Y. Y. Chu, Z. X. Huang, K. Liang, J. Guo, C. Boyer and J. T. Xu, A photocatalyst immobilized on fibrous and porous monolithic cellulose for heterogeneous catalysis of controlled radical polymerization, *Polym. Chem.*, 2018, **9**, 1666–1673, DOI: **10.1039/c7py01690e**.

78 L. Xia, B. F. Cheng, T. Y. Zeng, X. Nie, G. Chen, Z. Zhang, W. J. Zhang, C. Y. Hong and Y. Z. You, Polymer Nanofibers Exhibiting Remarkable Activity in Driving the Living Polymerization under Visible Light and Reusability, *Adv. Sci.*, 2020, **7**, 1902451, DOI: **10.1002/advs.201902451**.

79 J. J. Lessard, G. M. Scheutz, A. B. Korpusik, R. A. Olson, C. A. Figg and B. S. Sumerlin, Self-catalyzing photoredox polymerization for recyclable polymer catalysts, *Polym. Chem.*, 2021, **12**, 2205–2209, DOI: **10.1039/d1py00208b**.

80 X. F. Yang, A. Wang, B. Qiao, J. Li, J. Liu and T. Zhang, Single-Atom Catalysts: A New Frontier in Heterogeneous Catalysis, *Acc. Chem. Res.*, 2013, **46**, 1740–1748, DOI: **10.1021/ar300361m**.

81 A. Bagheri, C. M. Fellows and C. Boyer, Reversible Deactivation Radical Polymerization: From Polymer Network Synthesis to 3D Printing, *Adv. Sci.*, 2021, **8**, 202003701, DOI: **10.1002/advs.202003701**.

82 J. Cuthbert, A. C. Balazs, T. Kowalewski and K. Matyjaszewski, STEM Gels by Controlled Radical Polymerization, *Trends Chem.*, 2020, **2**, 341–353, DOI: **10.1016/j.trechm.2020.02.002**.

83 J. Cuthbert, A. Beziau, E. Gottlieb, L. Fu, R. Yuan, A. C. Balazs, T. Kowalewski and K. Matyjaszewski, Transformable Materials: Structurally Tailored and Engineered Macromolecular (STEM) Gels by Controlled Radical Polymerization, *Macromolecules*, 2018, **51**, 3808–3817, DOI: **10.1021/acs.macromol.8b00442**.

84 K. Matyjaszewski, Atom Transfer Radical Polymerization (ATRP): Current Status and Future Perspectives, *Macromolecules*, 2012, **45**, 4015–4039, DOI: **10.1021/ma3001719**.

85 F. Garcia-Martin, M. Quintanar-Audelo, Y. Garcia-Ramos, L. J. Cruz, C. Gravel, R. Furic, S. Cote, J. Tulla-Puche and F. Albericio, ChemMatrix, a poly(ethylene glycol)-based support for the solid-phase synthesis of complex peptides, *J. Comb. Chem.*, 2006, **8**, 213–220, DOI: **10.1021/cc0600019**.

86 Y. Garcia-Ramos, M. Paradis-Bas, J. Tulla-Puche and F. Albericio, ChemMatrix((R)) for complex peptides and combinatorial chemistry, *J. Pept. Sci.*, 2010, **16**, 675–678, DOI: **10.1002/psc.1282**.

87 G. Szczepaniak, K. Kapil, S. Adida, K. Kim, T.-C. Lin, G. Yilmaz, H. Murata and K. Matyjaszewski, Solid-Phase Synthesis of Well-Defined Multiblock Copolymers by Atom Transfer Radical Polymerization, *J. Am. Chem. Soc.*, 2024, **146**, 22247–22256, DOI: **10.1021/jacs.4c03675**.

88 Y. Cui, A. Taguchi, K. Kobayashi, H. Shida, K. Takayama, A. Taniguchi and Y. Hayashi, Use of solid-supported 4-fluorophenyl 3-nitro-2-pyridinesulfenate in the construction of disulfide-linked hybrid molecules, *Org. Biomol. Chem.*, 2020, **18**, 7094–7097, DOI: **10.1039/D0OB01370F**.

89 S. Mazzini, F. Garcia-Martin, M. Alvira, A. Avino, B. Manning, F. Albericio and R. Eritja, Synthesis of oligonucleotide derivatives using ChemMatrix supports, *Chem. Biodivers.*, 2008, **5**, 209–218, DOI: **10.1002/cbdv.200890012**.

90 G. Miralles, P. Verdie, K. Puget, A. Maurras, J. Martinez and G. Subra, Microwave-Mediated Reduction of Disulfide

Bridges with Supported (Tris(2-carboxyethyl)phosphine) as Resin-Bound Reducing Agent, *ACS Comb. Sci.*, 2013, **15**, 169–173, DOI: 10.1021/co300104k.

91 S. Averick, A. Simakova, S. Park, D. Konkolewicz, A. J. D. Magenau, R. A. Mehl and K. Matyjaszewski, ATRP under biologically relevant conditions: Grafting from a protein, *ACS Macro Lett.*, 2012, **1**, 6–10, DOI: 10.1021/mz200020c.

92 C. S. Cummings, A. S. Campbell, S. L. Baker, S. Carmali, H. Murata and A. J. Russell, Design of Stomach Acid-Stable and Mucin-Binding Enzyme Polymer Conjugates, *Biomacromolecules*, 2017, **18**, 576–586, DOI: 10.1021/acs.biomac.6b01723.

93 C. S. Cummings, K. Fein, H. Murata, R. L. Ball, A. J. Russell and K. A. Whitehead, ATRP-grown protein-polymer conjugates containing phenylpiperazine selectively enhance transepithelial protein transport, *J. Controlled Release*, 2017, **255**, 270–278, DOI: 10.1016/j.jconrel.2017.04.035.

94 B. S. Lele, H. Murata, K. Matyjaszewski and A. J. Russell, Synthesis of uniform protein-polymer conjugates, *Biomacromolecules*, 2005, **6**, 3380–3387, DOI: 10.1021/bm050428w.

95 S. L. Baker, B. Kaupbayeva, S. Lathwal, S. R. Das, A. J. Russell and K. Matyjaszewski, Atom Transfer Radical Polymerization for Biorelated Hybrid Materials, *Biomacromolecules*, 2019, **20**, 4272–4298, DOI: 10.1021/acs.biomac.9b01271.

96 S. L. Baker, A. Munasinghe, B. Kaupbayeva, N. R. Kang, M. Certiat, H. Murata, K. Matyjaszewski, P. Lin, C. M. Colina and A. J. Russell, Transforming protein-polymer conjugate purification by tuning protein solubility, *Nat. Commun.*, 2019, **10**, 4718, DOI: 10.1038/s41467-019-12612-9.

97 H. Murata, S. Carmali, S. L. Baker, K. Matyjaszewski and A. J. Russell, Solid-phase synthesis of protein-polymers on reversible immobilization supports, *Nat. Commun.*, 2018, **9**, 845, DOI: 10.1038/s41467-018-03153-8.

98 J. Cuthbert, S. V. Wanasinghe, K. Matyjaszewski and D. Konkolewicz, Are RAFT and ATRP Universally Interchangeable Polymerization Methods in Network Formation?, *Macromolecules*, 2021, **54**, 8331–8340, DOI: 10.1021/acs.macromol.1c01587.

99 S. DiLuzio, V. Mdluli, T. U. Connell, J. Lewis, V. VanBenschoten and S. Bernhard, High-Throughput Screening and Automated Data-Driven Analysis of the Triplet Photophysical Properties of Structurally Diverse, Heteroleptic Iridium(III) Complexes, *J. Am. Chem. Soc.*, 2021, **143**, 1179–1194, DOI: 10.1021/jacs.0c12290.

100 M. S. Lowry and S. Bernhard, Synthetically tailored excited states: Phosphorescent, cyclometalated iridium(III) complexes and their applications, *Chem. – Eur. J.*, 2006, **12**, 7970–7977, DOI: 10.1002/chem.200600618.

101 I. N. Mills, J. A. Porras and S. Bernhard, Judicious Design of Cationic, Cyclometalated Ir(III) Complexes for Photochemical Energy Conversion and Optoelectronics, *Acc. Chem. Res.*, 2018, **51**, 352–364, DOI: 10.1021/acs.accounts.7b00375.

102 F. Monti, A. Baschieri, L. Sambri and N. Armaroli, Excited-State Engineering in Heteroleptic Ionic Iridium(III) Complexes, *Acc. Chem. Res.*, 2021, **54**, 1492–1505, DOI: 10.1021/acs.accounts.0c00825.

103 Y. You, S. Cho and W. Nam, Cyclometalated Iridium(III) Complexes for Phosphorescence Sensing of Biological Metal Ions, *Inorg. Chem.*, 2014, **53**, 1804–1815, DOI: 10.1021/ic4013872.

104 K. K. W. Lo and K. Y. Zhang, Iridium(III) complexes as therapeutic and bioimaging reagents for cellular applications, *RSC Adv.*, 2012, **2**, 12069–12083, DOI: 10.1039/C2RA20967E.

105 E. Longhi and L. D. Cola, *Iridium(III) Complexes for OLED Application*, John Wiley & Sons Ltd, 1st edn, 2017. DOI: 10.1002/9781119007166.ch6.

106 B. F. DiSalle and S. Bernhard, Orchestrated Photocatalytic Water Reduction Using Surface-Adsorbing Iridium Photosensitizers, *J. Am. Chem. Soc.*, 2011, **133**, 11819–11821, DOI: 10.1021/ja201514e.

107 J. I. Goldsmith, W. R. Hudson, M. S. Lowry, T. H. Anderson and S. Bernhard, Discovery and high-throughput screening of heteroleptic iridium complexes for photoinduced hydrogen production, *J. Am. Chem. Soc.*, 2005, **127**, 7502–7510, DOI: 10.1021/ja0427101.

108 C. Ulbricht, B. Beyer, C. Friebe, A. Winter and U. S. Schubert, Recent Developments in the Application of Phosphorescent Iridium(III) Complex Systems, *Adv. Mater.*, 2009, **21**, 4418–4441, DOI: 10.1002/adma.200803537.

109 J. C. Deaton and F. N. Castellano, *Archetypal Iridium(III) Compounds for Optoelectronic and Photonic Applications*, John Wiley & Sons Ltd, 1st edn, 2017. DOI: 10.1002/9781119007166.

110 S. DiLuzio, T. U. Connell, V. Mdluli, J. F. Kowalewski and S. Bernhard, Understanding Ir(III) Photocatalyst Structure-Activity Relationships: A Highly Parallelized Study of Light-Driven Metal Reduction Processes, *J. Am. Chem. Soc.*, 2022, **144**, 1431–1444, DOI: 10.1021/jacs.1c12059.

111 E. Gottlieb, H. N. Kagalwala, J. Mohin, N. Budwal, S. Amsterdam, M. Lamson, K. Matyjaszewski, S. Bernhard and T. Kowalewski, Common Carbons as Water-Reducing Catalysts in Photo-Driven Hydrogen Evolution with Nitrogen-Dependent Activity, *ChemNanoMat*, 2018, **4**, 1039–1042, DOI: 10.1002/cnma.201800167.

112 V. Mdluli, S. Diluzio, J. Lewis, J. F. Kowalewski, T. U. Connell, D. Yaron, T. Kowalewski and S. Bernhard, High-throughput Synthesis and Screening of Iridium(III) Photocatalysts for the Fast and Chemoselective Dehalogenation of Aryl Bromides, *ACS Catal.*, 2020, **10**, 6977–6987, DOI: 10.1021/acscatal.0c02247.

113 F. Dumur, D. Gigmes, J. P. Fouassier and J. Lalevé, Organic Electronics: An El Dorado in the Quest of New Photocatalysts for Polymerization Reactions, *Acc. Chem. Res.*, 2016, **49**, 1980–1989, DOI: 10.1021/acs.accounts.6b00227.

114 B. P. Fors and C. J. Hawker, Control of a Living Radical Polymerization of Methacrylates by Light, *Angew. Chem., Int. Ed.*, 2012, **51**, 8850–8853, DOI: **10.1002/anie.201203639**.

115 V. Kottisch, M. J. Supej and B. P. Fors, Enhancing Temporal Control and Enabling Chain-End Modification in Photoregulated Cationic Polymerizations by Using Iridium-Based Catalysts, *Angew. Chem., Int. Ed.*, 2018, **57**, 8260–8264, DOI: **10.1002/ange.201804111**.

116 G. Anilkumar, H. Nambu and Y. Kita, A simple and efficient iodination of alcohols on polymer-supported triphenylphosphine, *Org. Process Res. Dev.*, 2002, **6**, 190–191, DOI: **10.1021/op010094c**.

117 C. G. Wang and A. Goto, Solvent-Selective Reactions of Alkyl Iodide With Sodium Azide for Radical Generation and Azide Substitution and Their Application to One-Pot Synthesis of Chain-End-Functionalized Polymers, *J. Am. Chem. Soc.*, 2017, **139**, 10551–10560, DOI: **10.1021/jacs.7b05879**.

118 M. Meldal and C. W. Tornoe, Cu-catalyzed azide-alkyne cycloaddition, *Chem. Rev.*, 2008, **108**, 2952–3015, DOI: **10.1021/cr0783479**.

119 N. Y. Chau, P. Y. Ho, C. L. Ho, D. Ma and W. Y. Wong, Color-tunable thiazole-based iridium(III) complexes: Synthesis, characterization and their OLED applications, *J. Organomet. Chem.*, 2017, **829**, 92–100, DOI: **10.1016/j.jorganchem.2016.11.018**.